THE JOURNAL OF PHYSICAL CHEMISTRY C

Article

Cite This: J. Phys. Chem. C 2017, 121, 24179-24184

pubs.acs.org/JPCC

VS_2/Graphene Heterostructures as Promising Anode Material for Li-Ion Batteries

Natalia S. Mikhaleva,[†] Maxim A. Visotin,*[,†,§] Aleksandr A. Kuzubov,[†] and Zakhar I. Popov[‡,§]

[†]Siberian Federal University, 79 Svobodny av., Krasnoyarsk, 660041, Russian Federation

[‡]National University of Science and Technology MISiS, 4 Leninskiy prospekt, Moscow, 119049, Russian Federation

[§]Kirensky Institute of Physics, 50/38 Akademgorodok, Krasnoyarsk, 660036, Russian Federation

Supporting Information

ABSTRACT: Two-layer freestanding heterostructure consisting of VS_2 monolayer and graphene was investigated by means of density functional theory computations as a promising anode material for lithium-ion batteries (LIB). We have investigated lithium atoms' sorption and diffusion on the surface and in the interface layer of VS_2/graphene heterostructure with both H and T configurations of VS_2 monolayer. The theoretically predicted capacity of VS_2/graphene heterostructures is high (569 mAh/g), and the diffusion barriers are considerably lower for the heterostructures than for bulk VS_2, so that they are comparable to barriers in graphitic LIB anodes (~0.2 eV). Our results suggest that VS_2/graphene heterostructures can be used as a promising anode material for lithium-ion batteries with high power density and fast charge/discharge rates.

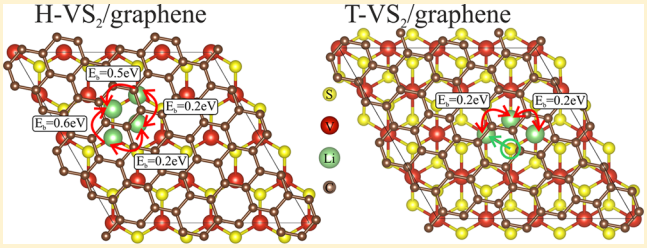

INTRODUCTION

Li-ion batteries (LIB) are the most popular power sources for mobile electronic devices. The main advantages of these batteries are big specific capacity, high efficiency, long lifetime, and operational safety. On the other hand, a growing level of requirements and an expansion of application fields raise new challenges for the accumulators and the electrode materials used. A big number of recent investigations[1−5] focus on the search for new active anode materials or, alternatively, the way to enhance the properties of known materials by modification and nanostructure design.

Having high specific surface area, electroconductivity, and elastic moduli,[6] graphene appears to be a promising material base for power storage devices. However, Liu et al.[7] have shown that pure graphene-based lithium storage matrices suffer from negative effects while lithium clusterization and phase separation occur. Despite that, graphene sheets were successfully used as anode material in Li-ion accumulators and were confirmed to exhibit good electrochemical properties.[8,9] Also, BC_3, a graphene-derived material, is also a very promising anode material.[7,10]

Along with graphene, planar transition metal compounds have been extensively investigated recently. Unique properties, due to the layered structure, high specific surface area, and presence of d-electrons, provide 2D transition metal materials, such as oxides and dichalcogenides, with important applications in different fields of nanoelectronics.[11−17] Series of investigations have shown monolayers of molybdenum disulfide as a prospective anode material for LIB with good performance and remarkable specific capacity.[18−20] However, despite low lithium diffusion barriers and high capacity,[21] MoS_2 is a semiconductor with a significant band gap of 1.8 eV, which considerably affects the material's electrochemical properties. Opposed to MoS_2 nanosheets, zigzag-type nanoribbons exhibit metallic conductance[22,23] and high lithium mobility at the surface, although lithium is bounded stronger than to nanosheets.[21] However, commercial-scale MoS_2 nanoribbon production is currently an unpromising problem.

Another prospective electrode material is vanadium disulfide (VS_2). Intercalation of VS_2 by Li^+ was first done in 1977 by Murphy et al.,[24] and later, it was suggested as a cathode for LIB.[25,26] As an anode material, $Li_{0.8}VS_2$ was tested in refs 27 and 28, where the specific capacity was found to be lower than 200 mAh/g. Once again, VS_2 attracted attention after its 2D conductive phase was synthesized and then used in a supercapacitor with big specific capacity and high cycling stability.[29,30] A theoretical study in ref 31 proposed VS_2 monolayer as a material for LIB anode. Lithium atoms are easily adsorbed on the monolayer surface with the maximal theoretical capacity of 466 mAh/g (corresponding to Li_2VS_2) and with the diffusion rates higher than in graphite and MoS_2.

Having the unique properties of graphene and transition-metal oxides and dichalcogenides, composites and heterostructures based on these compounds are expected to have even more promising capabilities. Advances in properties of graphene/transition-metal dichalcogenide (oxide) nanocomposites may result from a variety of factors, such as changes in morphology and chemical composition,[32] tuning of electronic

Received: August 2, 2017
Revised: September 21, 2017
Published: October 4, 2017

DOI: 10.1021/acs.jpcc.7b07630
J. Phys. Chem. C 2017, 121, 24179−24184

transport, increase in number of active states, and buffering due to volumetric expansion.[33−39] Composites of graphene and MoS_2 have been studied in detail,[40−43] including their performance as LIB anode, for example, MoS_2/rGO (reduced graphene oxide) has specific capacity of 1300 mAh/g, high-rate capability, and cycling stability.[40]

Earlier, a composite consisting of the VS_2 flakes with 50 nm thickness on graphene nanosheets (VS_2/GNS) was obtained and investigated as LIB anode and cathode material by Fang et al.[44] The VS_2/GNS nanocomposites have shown good characteristics as a cathode material both at high and low charging rates with initial capacity of 180.1 mAh/g. As anode material, VS_2/GNS exhibits good reversible performance with 528 mAh/g capacity even after 100 cycles at 200 mA/g. It was suggested that interactions between the graphene and VS_2 provide both good electron transport and mechanical strengthening resulting in excellent electrochemical properties. The VS_2/GNS composites may be promising electrode materials for the next generation of rechargeable lithium ion batteries and need further investigations including investigation of lithiation processes at the atomic scale in order to understand the mechanism of lithium penetration. A major limitation of the work was that the monolayer thickness was not achieved; by reducing the number of stacked VS_2 layers, the sorption properties of the composite may improve.

Another concern is the material degradation. Metal dichalcogenides' inclination for aging with structural degeneration was shown recently.[45−47] As a proposed countermeasure, combining the dichalcogenide monolayer into a heterostructure with an inert outer layer, such as graphene or h-BN,[48] can prevent aging and can preserve the unique properties.

This article is devoted to a study of lithium sorption and diffusion in freestanding VS_2/graphene heterostructure. Sorption energies and diffusion barriers on the surface and in the interlayer space of the heterostructure are calculated and compared against bulk systems.

CALCULATION METHODS

In this work, the properties of VS_2/graphene heterosturucture are investigated by means of quantum-chemical modeling within the framework of density functional theory (DFT)[49,50] using plane-wave basis set and the projector augmented wave (PAW) method[51,52] as implemented in VASP.[53−55] Generalized gradient approximation (GGA) was used in the form of PBE (Perdew−Burke−Ernzerhof) exchange-correlation functional[56] as well as the Grimme dispersion corrections for van der Waals interaction description (DFT-D3).[57] For exploring transition states and potential energy barrier calculations of lithium atom passing from one position to another, the nudged elastic band method (NEB)[58] was used.

For the Brillouin zone sampling, the gamma-centered Monkhorst−Pack scheme[59] was chosen. The plane wave basis cutoff energy E_{cutoff} = 400 eV was used. While the periodic boundary conditions are necessarily applied to simulation cells in the plane wave basis, one has to separate the monolayers from the periodic images in the neighboring cells in order to model an isolated 2D structure. For this purpose, a vacuum spacing of 20 Å perpendicular to the monolayer's plane was made in the simulation cell. In all geometry optimizations, the convergence criterion was so that the maximal force acting on any atom was less than 0.01 eV/Å. All structures were visualized in VESTA.[60]

RESULTS AND DISCUSSION

First, full geometry optimization was carried out for VS_2 unit cells of two possible phases: trigonal-prismatic (H) and octahedral (T). As in our previous work,[61] in the absence of available experimental data for VS_2 monolayers, we have also conducted bulk geometry calculations, and the results for bulk 1T-VS_2, obtained at the DFT-D3 level of theory ($a = b$ = 3.16 Å, c = 5.79 Å), coincide well with those from the experiment ($a = b$ = 3.23 Å, c = 5.71 Å).[62] The equilibrium monolayer lattice constants are 3.17 and 3.16 Å for the T and H phases, respectively, at the PBE with DFT-D3 level of theory.

Next, vertical VS_2/graphene heterostructures were constructed to simulate single lithium atom sorption in the heterostructures and to compare it with sorption on VS_2 monolayer surface. The model of VS_2/graphene heterostructures was adopted from ref 61, where VS_2 and graphene layers were stacked with a misorientation angle β = 20 between in-plane lattice vectors of the layers. For this, $\sqrt{7} \times \sqrt{7}$ graphene supercell was placed over 2 × 2 supercell of VS_2. This cell was used for calculation of higher lithium concentrations, while for low lithium concentrations and particularly for calculation of potential barriers, the cell was doubled in plane in two directions. The dimensions of the k-point mesh were set to 12 × 12 × 1 for calculations in the smaller simulation cell and to 6 × 6 × 1 for the doubled cell. Using these supercells, the most preferable sites for lithium sorption on VS_2 surface (sites H, S, and V) and in the interface region between the layers of graphene and VS_2 (sites 1−4) were determined (see Figure 1, Table 1).

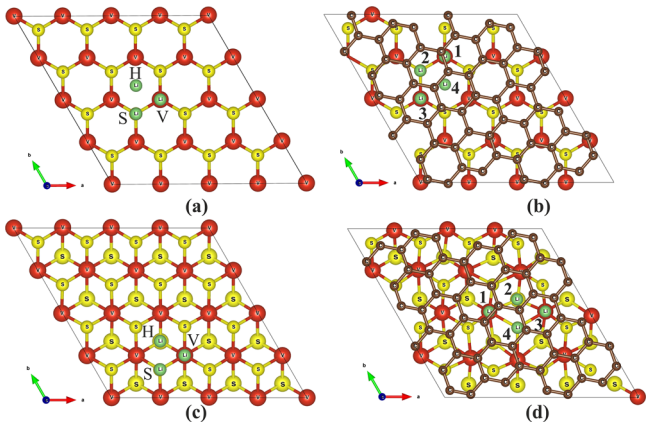

Figure 1. Lithium atom sites on VS_2 surface: (a) H-VS_2, (c) T-VS_2; in between graphene and VS_2: (b) H-VS_2, (d) T-VS_2.

The sorption energy of lithium on stand-alone VS_2 monolayer or the heterostructure was calculated as

$$E_{sorp} = (E_{total} - E_{substrate} - nE_{Li})/n \quad (1)$$

where E_{total} is the full energy of the substrate (monolayer or heterostructure) with lithium atoms on it, $E_{substrate}$ is the energy of the substrate without adatoms, E_{Li} is the energy of one atom in lithium crystal, and n is the number of Li atoms adsorbed on the substrate.

According to the calculated sorption energies of the single lithium atom, on the surface of VS_2 and in the interface region of VS_2/graphene as well, the most energetically preferable sites are above the vanadium atom (site V) for both T and H phases (see Figure 1 and Table 1).

DOI: 10.1021/acs.jpcc.7b07630
J. Phys. Chem. C 2017, 121, 24179−24184

Table 1. Structural and Magnetic Properties of the Heterostructures with Single Li Adatom in Different Positions

Li position		sorption energy, eV	magnetization, μ_B per u.c.	bond length, Å		
				Li−V	Li−S	Li−C
		H-VS_2				
between graphene and VS_2	1	−1.99	12.60	2.91	2.35	2.29
	3	−1.98	12.62	2.97	2.38	2.39
	4	−1.94	12.64	3.45	2.36	2.34
	2	−1.48	12.77	3.65	2.19	2.23
on VS_2 surface	V	−2.01	12.53	2.94	2.36	
	H	−1.96	12.55	3.47	2.37	
	S	−1.32	12.63	4.09	2.21	
		T-VS_2				
between graphene and VS_2	1	−1.84	3.72	2.78	2.31	2.36
	2 (went to 1)	−1.84	3.72	2.78	2.31	2.36
	3	−1.81	3.86	2.84	2.32	2.52
	4	−1.77	4.18	2.74	2.27	2.34
on VS_2 surface	V	−1.87	3.82	2.79	2.31	
	H	−1.84	3.72	3.27	2.28	
	S	−1.41	4.18	3.96	2.19	

The tendency is the same for the stand-alone VS_2 monolayers (see Figure 1); however, the energies of sorption on the heterostructure are higher. The sorption energy for positions V, H, and S of Li atom is equal to −1.82, −1.74, and −1.17 eV for H-VS_2 monolayer and to −1.56, −1.44, and −0.88 eV for T-VS_2 monolayer, respectively. The occupation of the site V is more energetically favorable in both cases. As for the sorption between graphene and VS_2, the differences in sorption energy in the sites 1, 3, and 4 are negligible for both phases; however, the absolute values of E_{sorp} are higher for the H phase. The position 2 for the T phase is unstable, and the Li atom went from 2 to 1 during the geometry optimization.

One can speculate about a correlation between the distance from the lithium atom to the nearest vanadium atom and the sorption energy. The smaller the distance to vanadium, the higher the sorption energy for both H and T phases. The distance from lithium to graphene varies insignificantly and does not contribute to the changes in sorption energy. There is no significant effect on the magnetic properties of vanadium disulfide by adsorbed lithium atom at the PBE level of theory.

Further, single Li diffusion was modeled for the interface region of VS_2/graphene (Figure 2c, d) and, for comparison, on the surface of VS_2 monolayer (Figure 2a, b); the influence of underlying graphene on the corresponding barriers in the heterostructures is negligible. For diffusion on the surface of both T and H phases, the easiest way for Li atom diffusion is V−H−V; however, the barrier height for the V−H−V transition is a bit lower for the H-VS_2 phase (0.18 eV) than for the T-VS_2 phase (0.23 eV). The results are consistent with the previous calculations,[63] where the potential barriers for the H phase monolayer were obtained.

The diffusion of Li atom in the interface region of T-VS_2/graphene heterostructure is limited by the 1−4 transition (Figure 2d). For the H-VS_2/graphene heterostructure, the most preferable diffusion path is 1−4−3 (Figure 2c). In that, the barriers of 1−4, 4−3, and V−H transitions are almost equal, so that the diffusion in between the layers and on the surface may proceed with equal rates.

The diffusion barriers inside the interface region of the VS_2/graphene heterostructure are lower than the barriers in bulk T-VS_2 (which were previously estimated as 0.24 eV[63]) and are comparable to the barriers in graphite, the most popular LIB anode material.[64] Thus, the combination of VS_2 with graphene makes up a prospective material with good lithium capacity, remarkable electronic conductance, and high sorption/desorption rates.

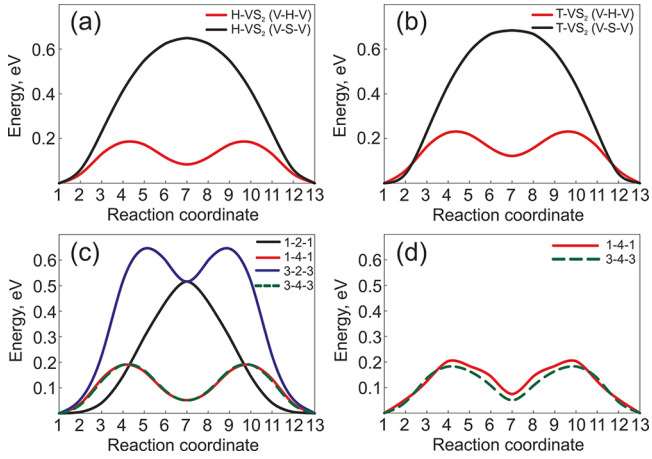

Figure 2. Transition barriers between local minima for single lithium atom on the surface of (a) H-VS_2 monolayer and (b) T-VS_2 monolayer and in the interlayer space between graphene and (c) H-VS_2 and (d) T-VS_2.

As the energy barriers for Li atom transitions in the interface region of the heterostructures are low, it should be easy for lithium to diffuse in the interlayer space. Next, the maximal amount of lithium x, that can be sorbed in between graphene and VS_2 ($VS_2/Li_x/C_{3.5}$), was determined using the bigger simulation cell for $x < 0.25$ and the smaller cell for higher concentration. It was assumed that Li atoms occupy the most preferable sites in the interface region, that is, above vanadium atoms. Descriptions of all the concentrations considered and the lithium atom distributions can be found in the Supporting Information, Figures S1 and S2. According to the results (see Figure 3), the sorption energies increase monotonically with the amount of lithium inside the interface region. The maximal amount of lithium that can be sorbed in the interface region of VS_2/graphene heterostructures is 1.75 Li atoms per VS_2 unit, and further filling of the structure leads to the positive values of the sorption energies, which means that higher lithium content

DOI: 10.1021/acs.jpcc.7b07630
J. Phys. Chem. C 2017, 121, 24179−24184

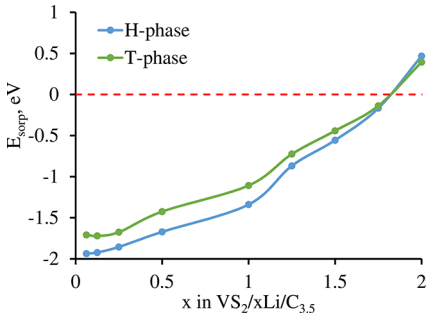

Figure 3. Sorption energy of Li in VS_2/graphene heterostructure depending on amounts of Li atoms in the interlayer space.

is energetically unfavorable. The increase in sorption energies comes from Coulomb repulsion between positively charged Li atoms that are placed in closed space between the layers. This also explains well the vanishing difference between the sorption energies in the H and T phases. The difference in the geometry of the second (outer) layer of sulfur atoms is only noticeable at low Li concentrations and is obscured by the short-range repulsion forces.

The density of 1.75 Li atoms per VS_2 unit stored in between the layers of the heterostructure is significantly higher than the capacity between the layers of bulk T-VS_2 (1 Li atom per formula unit) or graphite (0.166 Li atoms per carbon atom) and is even higher than the sum of these capacities. A possible reason for the enhanced capacity of the interface is the following. The energy of lithium sorption on any substrate can be divided into three parts: attraction of Li atoms to the substrate, mutual repulsion of Li atoms, and deformation of the substrate. The first term does not change significantly from the bulk VS_2 (or graphene) to the case of the heterostructure, but the third part should have a considerable impact on the overall sorption energy. A rough estimate of the difference in the deformation energies can be obtained by estimating the binding energies between layers in VS_2 or graphene. The energy needed to pull apart the monolayers in the heterostructure is 0.35 eV per cell. According to our calculations, for the cell of the same size, one needs 0.69 eV to pull apart the layers of bigraphene. In case of two-layered T-VS_2, the energy is 1.00 eV.

Thus, the maximal possible lithium content in the interlayer region corresponds to a formula $VS_2/Li_{1.75}/C_{3.5}$. Taking into account sorption on the outer surface of VS_2 monolayer and graphene[31] with formation of $Li/VS_2/Li_{1.75}/C_{3.5}/Li_{0.583}$, the overall capacity can reach a value of 569 mAh/g. This is close to the experimentally obtained capacity of 528 mAh/g after 100 cycles for multilayered VS_2/GNS nanocomposites[44] and is much higher than the theoretically possible 466 mAh/g[31] for VS_2 monolayer. Also, no chemical bonds are broken during the lithiation up to this concentration, which argues for good reversibility of this process. However, if chemical transformations were considered for the heterostructure, the amount of lithium able to be sorbed could be even higher than 569 mAh/g.

Importantly, during the lithiation, the heterostructure retains its graphene-inhereted transport properties. The calculated partial densities of states (pDOS) from the carbon atoms show linear sections corresponding to the Dirac cones insignificantly affected by the impurity states coming from Li−C interactions. The vertex of the cone is not overlapped by any other bands, although it is shifted 1.4 eV downward (for x = 1) in accordance with n-doping of the graphene monolayer by the electrons transferred from lithium atoms (Figure S3).

CONCLUSIONS

Quantum-chemical calculations show that lithium can be effectively adsorbed on the surface as well as in the interplanar space of VS_2/graphene heterostructures with the sorption energies similar to those for bulk T-VS_2 (~2 eV). However, the diffusion barriers are considerably lower for the heterostructures and are comparable to barriers in graphitic LIB anodes (~0.2 eV).

The sorption energies become positive only when 1.75 monolayers of Li atoms per VS_2 are sorbed in the interface region of the heterostructure. This results in overall lithium capacity of 569 mAh/g which agrees well with the recently reported experimental results.

Thus, the combination of VS_2 monolayer with graphene makes up a prospective material with good lithium capacity, remarkable electronic conductance, and high sorption/desorption rates.

ASSOCIATED CONTENT

Supporting Information

The Supporting Information is available free of charge on the ACS Publications website at DOI: 10.1021/acs.jpcc.7b07630.

Atomic structures of VS_2/graphene heterostructure with different amounts of Li atoms in the interlayer space and partial DOS of graphene in $VS_2/Li/C_{3.5}$ for both H and T phases of VS_2 (PDF)

AUTHOR INFORMATION

Corresponding Author

*E-mail: visotin.maxim@gmail.com. Phone: +7-983-500-67-70.

ORCID

Maxim A. Visotin: 0000-0003-2265-9394

Notes

The authors declare no competing financial interest.

ACKNOWLEDGMENTS

We thank the Information Technology Centre of Novosibirsk State University for providing access to cluster computational resources. This work was supported by the government contract of the Ministry of Education and Science of the Russian Federation to Siberian Federal University (Grant No. 16.1455.2017/PCh). N. S. M. acknowledges the financial support of the RFBR, through the research project No. 16-32-60003 mol_a_dk. M. A. V. acknowledges the financial support of the RFBR, through the research project No. 16-32-00252 mol_a. Z. I. P. gratefully acknowledges the financial support of the Ministry of Education and Science of the Russian Federation in the framework of Increase Competitiveness Program of NUST ≪MISiS≫ (No. K2-2017-001) and the support of the RFBR through the research project No. 17-42-190308 r_a.

REFERENCES

(1) Tarascon, J.-M.; Armand, M. Issues and Challenges Facing Rechargeable Lithium Batteries. *Nature* **2001**, *414*, 359−367.

(2) Sides, C. R.; Martin, C. R. Nanostructured Electrodes and the Low-Temperature Performance of Li-Ion Batteries. *Adv. Mater.* **2005**, *17*, 125−128.

(3) Armand, M.; Tarascon, J.-M. Building Better Batteries. *Nature* **2008**, *451*, 652−657.
(4) Etacheri, V.; Marom, R.; Elazari, R.; Salitra, G.; Aurbach, D. Challenges in the Development of Advanced Li-Ion Batteries: A Review. *Energy Environ. Sci.* **2011**, *4*, 3243.
(5) Liu, N.; Li, W.; Pasta, M.; Cui, Y. Nanomaterials for Electrochemical Energy Storage. *Front. Phys.* **2014**, *9*, 323−350.
(6) Zhou, G.; Li, F.; Cheng, H.-M. Progress in Flexible Lithium Batteries and Future Prospects. *Energy Environ. Sci.* **2014**, *7*, 1307−1338.
(7) Liu, Y.; Artyukhov, V. I.; Liu, M.; Harutyunyan, A. R.; Yakobson, B. I. Feasibility of Lithium Storage on Graphene and Its Derivatives. *J. Phys. Chem. Lett.* **2013**, *4*, 1737−1742.
(8) Liu, J.; Liu, X.-W. Two-Dimensional Nanoarchitectures for Lithium Storage. *Adv. Mater.* **2012**, *24*, 4097−4111.
(9) Lian, P.; Zhu, X.; Liang, S.; Li, Z.; Yang, W.; Wang, H. Large Reversible Capacity of High Quality Graphene Sheets as an Anode Material for Lithium-Ion Batteries. *Electrochim. Acta* **2010**, *55*, 3909−3914.
(10) Kuzubov, A. A.; Fedorov, A. S.; Eliseeva, N. S.; Tomilin, F. N.; Avramov, P. V.; Fedorov, D. G. High-Capacity Electrode Material BC_3 for Lithium Batteries Proposed by Ab Initio Simulations. *Phys. Rev. B: Condens. Matter Mater. Phys.* **2012**, *85*, 195415.
(11) Johari, P.; Shenoy, V. B. Tuning the Electronic Properties of Semiconducting Transition Metal Dichalcogenides by Applying Mechanical Strains. *ACS Nano* **2012**, *6*, 5449−5456.
(12) Eda, G.; Yamaguchi, H.; Voiry, D.; Fujita, T.; Chen, M.; Chhowalla, M. Photoluminescence from Chemically Exfoliated MoS_2. *Nano Lett.* **2011**, *11*, 5111−5116.
(13) Xu, M.; Liang, T.; Shi, M.; Chen, H. Graphene-Like Two-Dimensional Materials. *Chem. Rev.* **2013**, *113*, 3766−3798.
(14) Wang, Q. H.; Kalantar-Zadeh, K.; Kis, A.; Coleman, J. N.; Strano, M. S. Electronics and Optoelectronics of Two-Dimensional Transition Metal Dichalcogenides. *Nat. Nanotechnol.* **2012**, *7*, 699−712.
(15) Song, C.; Yu, K.; Yin, H.; Fu, H.; Zhang, Z.; Zhang, N.; Zhu, Z. Highly Efficient Field Emission Properties of a Novel Layered VS_2/ZnO Nanocomposite and Flexible VS_2 Nanosheet. *J. Mater. Chem. C* **2014**, *2*, 4196−4202.
(16) Choi, S. H.; Kang, Y. C. Sodium Ion Storage Properties of WS_2 -Decorated Three-Dimensional Reduced Graphene Oxide Microspheres. *Nanoscale* **2015**, *7*, 3965−3970.
(17) Puthussery, J.; Seefeld, S.; Berry, N.; Gibbs, M.; Law, M. Colloidal Iron Pyrite (FeS_2) Nanocrystal Inks for Thin-Film Photovoltaics. *J. Am. Chem. Soc.* **2011**, *133*, 716−719.
(18) Du, G.; Guo, Z.; Wang, S.; Zeng, R.; Chen, Z.; Liu, H. Superior Stability and High Capacity of Restacked Molybdenum Disulfide as Anode Material for Lithium Ion Batteries. *Chem. Commun.* **2010**, *46*, 1106−1108.
(19) Ding, S.; Zhang, D.; Chen, J. S.; Lou, X. W. (David). Facile Synthesis of Hierarchical MoS_2 Microspheres Composed of Few-Layered Nanosheets and Their Lithium Storage Properties. *Nanoscale* **2012**, *4*, 95−98.
(20) Hwang, H.; Kim, H.; Cho, J. MoS_2 Nanoplates Consisting of Disordered Graphene-like Layers for High Rate Lithium Battery Anode Materials. *Nano Lett.* **2011**, *11*, 4826−4830.
(21) Li, Y.; Wu, D.; Zhou, Z.; Cabrera, C. R.; Chen, Z. Enhanced Li Adsorption and Diffusion on MoS_2 Zigzag Nanoribbons by Edge Effects: A Computational Study. *J. Phys. Chem. Lett.* **2012**, *3*, 2221−2227.
(22) Li, Y.; Zhou, Z.; Zhang, S.; Chen, Z. MoS_2 Nanoribbons: High Stability and Unusual Electronic and Magnetic Properties. *J. Am. Chem. Soc.* **2008**, *130*, 16739−16744.
(23) Wang, Z.; Li, H.; Liu, Z.; Shi, Z.; Lu, J.; Suenaga, K.; Joung, S.-K.; Okazaki, T.; Gu, Z.; Zhou, J.; et al. Mixed Low-Dimensional Nanomaterial: 2D Ultranarrow MoS_2 Inorganic Nanoribbons Encapsulated in Quasi-1D Carbon Nanotubes. *J. Am. Chem. Soc.* **2010**, *132*, 13840−13847.
(24) Murphy, D. W.; Carides, J. N.; Di Salvo, F. J.; Cros, C.; Waszczak, J. V. Cathodes for Nonaqueous Lithium Batteries Based on VS_2. *Mater. Res. Bull.* **1977**, *12*, 825−830.
(25) Murphy, D. W.; Di Salvo, F. J.; Carides, J. N. Vanadium Disulfide: Metal Substitution and Lithium Intercalation. *J. Solid State Chem.* **1979**, *29*, 339−343.
(26) Vadivel Murugan, A.; Quintin, M.; Delville, M.-H.; Campet, G.; Vijayamohanan, K. Entrapment of poly(3,4-Ethylenedioxythiophene) between VS_2 Layers to Form a New Organic-Inorganic Intercalative Nanocomposite. *J. Mater. Chem.* **2005**, *15*, 902−909.
(27) GUZMÁN, R.; LAVELA, P.; MORALES, J.; TIRADO, J. L. $VSe_{2-y}S_y$ Electrodes in Lithium and Lithium-Ion Cells. *J. Appl. Electrochem.* **1997**, *27*, 1207−1211.
(28) Kim, Y.; Park, K.; Song, S.; Han, J.; Goodenough, J. B. Access to M^{3+}/M^{2+} Redox Couples in Layered $LiMS_2$ Sulfides (M = Ti, V, Cr) as Anodes for Li-Ion Battery. *J. Electrochem. Soc.* **2009**, *156*, A703.
(29) Feng, J.; Sun, X.; Wu, C.; Peng, L.; Lin, C.; Hu, S.; Yang, J.; Xie, Y. Metallic Few-Layered VS_2 Ultrathin Nanosheets: High Two-Dimensional Conductivity for In-Plane Supercapacitors. *J. Am. Chem. Soc.* **2011**, *133*, 17832−17838.
(30) Feng, J.; Peng, L.; Wu, C.; Sun, X.; Hu, S.; Lin, C.; Dai, J.; Yang, J.; Xie, Y. Giant Moisture Responsiveness of VS_2 Ultrathin Nanosheets for Novel Touchless Positioning Interface. *Adv. Mater.* **2012**, *24*, 1969−1974.
(31) Jing, Y.; Zhou, Z.; Cabrera, C. R.; Chen, Z. Metallic VS_2 Monolayer: A Promising 2D Anode Material for Lithium Ion Batteries. *J. Phys. Chem. C* **2013**, *117*, 25409−25413.
(32) Rout, C. S.; Kim, B.-H.; Xu, X.; Yang, J.; Jeong, H. Y.; Odkhuu, D.; Park, N.; Cho, J.; Shin, H. S. Synthesis and Characterization of Patronite Form of Vanadium Sulfide on Graphitic Layer. *J. Am. Chem. Soc.* **2013**, *135*, 8720−8725.
(33) Chang, K.; Chen, W. l-Cysteine-Assisted Synthesis of Layered MoS_2 /Graphene Composites with Excellent Electrochemical Performances for Lithium Ion Batteries. *ACS Nano* **2011**, *5*, 4720−4728.
(34) Xiang, Q.; Yu, J.; Jaroniec, M. Synergetic Effect of MoS_2 and Graphene as Cocatalysts for Enhanced Photocatalytic H_2 Production Activity of TiO_2 Nanoparticles. *J. Am. Chem. Soc.* **2012**, *134*, 6575−6578.
(35) Wang, R.; Xu, C.; Sun, J.; Liu, Y.; Gao, L.; Lin, C. Free-Standing and Binder-Free Lithium-Ion Electrodes Based on Robust Layered Assembly of Graphene and Co_3O_4 Nanosheets. *Nanoscale* **2013**, *5*, 6960.
(36) Wang, G. X.; Bewlay, S.; Yao, J.; Liu, H. K.; Dou, S. X. Tungsten Disulfide Nanotubes for Lithium Storage. *Electrochem. Solid-State Lett.* **2004**, *7*, A321.
(37) Feng, C.; Huang, L.; Guo, Z.; Liu, H. Synthesis of Tungsten Disulfide (WS_2) Nanoflakes for Lithium Ion Battery Application. *Electrochem. Commun.* **2007**, *9*, 119−122.
(38) Xu, C.; Zeng, Y.; Rui, X.; Xiao, N.; Zhu, J.; Zhang, W.; Chen, J.; Liu, W.; Tan, H.; Hng, H. H.; et al. Controlled Soft-Template Synthesis of Ultrathin C@FeS Nanosheets with High-Li-Storage Performance. *ACS Nano* **2012**, *6*, 4713−4721.
(39) Guo, J.; Li, F.; Sun, Y.; Zhang, X.; Tang, L. Graphene-Encapsulated Cobalt Sulfides Nanocages with Excellent Anode Performances for Lithium Ion Batteries. *Electrochim. Acta* **2015**, *167*, 32−38.
(40) Chang, K.; Chen, W. In Situ Synthesis of MoS_2/Graphene Nanosheet Composites with Extraordinarily High Electrochemical Performance for Lithium Ion Batteries. *Chem. Commun.* **2011**, *47*, 4252−4254.
(41) Zhu, C.; Mu, X.; van Aken, P. A.; Maier, J.; Yu, Y. Fast Li Storage in MoS_2 -Graphene-Carbon Nanotube Nanocomposites: Advantageous Functional Integration of 0D, 1D, and 2D Nanostructures. *Adv. Energy Mater.* **2015**, *5*, 1401170.
(42) Xiao, J.; Wang, X.; Yang, X.-Q.; Xun, S.; Liu, G.; Koech, P. K.; Liu, J.; Lemmon, J. P. Electrochemically Induced High Capacity Displacement Reaction of PEO/MoS_2/Graphene Nanocomposites with Lithium. *Adv. Funct. Mater.* **2011**, *21*, 2840−2846.

DOI: 10.1021/acs.jpcc.7b07630
J. Phys. Chem. C 2017, 121, 24179−24184

(43) Zhou, X.; Wan, L.-J.; Guo, Y.-G. Facile Synthesis of MoS_2@CMK-3 Nanocomposite as an Improved Anode Material for Lithium-Ion Batteries. *Nanoscale* **2012**, *4*, 5868.
(44) Fang, W.; Zhao, H.; Xie, Y.; Fang, J.; Xu, J.; Chen, Z. Facile Hydrothermal Synthesis of VS_2 /Graphene Nanocomposites with Superior High-Rate Capability as Lithium-Ion Battery Cathodes. *ACS Appl. Mater. Interfaces* **2015**, *7*, 13044−13052.
(45) Mahalu, D.; Peisach, M.; Jaegermann, W.; Wold, A.; Tenne, R. Controlled Photocorrosion of Tungsten Diselenide: Influence of Molecular Oxygen. *J. Phys. Chem.* **1990**, *94*, 8012−8013.
(46) Parzinger, E.; Miller, B.; Blaschke, B.; Garrido, J. A.; Ager, J. W.; Holleitner, A.; Wurstbauer, U. Photocatalytic Stability of Single- and Few-Layer MoS_2. *ACS Nano* **2015**, *9*, 11302−11309.
(47) Chang, Y.-H.; Zhang, W.; Zhu, Y.; Han, Y.; Pu, J.; Chang, J.-K.; Hsu, W.-T.; Huang, J.-K.; Hsu, C.-L.; Chiu, M.-H.; et al. Monolayer $MoSe_2$ Grown by Chemical Vapor Deposition for Fast Photodetection. *ACS Nano* **2014**, *8*, 8582−8590.
(48) Ahn, S.; Kim, G.; Nayak, P. K.; Yoon, S. I.; Lim, H.; Shin, H.-J.; Shin, H. S. Prevention of Transition Metal Dichalcogenide Photodegradation by Encapsulation with H-BN Layers. *ACS Nano* **2016**, *10*, 8973−8979.
(49) Hohenberg, P.; Kohn, W. Inhomogeneous Electron Gas. *Phys. Rev.* **1964**, *136*, B864−B871.
(50) Kohn, W.; Sham, L. J. Self-Consistent Equations Including Exchange and Correlation Effects. *Phys. Rev.* **1965**, *140*, A1133−A1138.
(51) Blöchl, P. E. Projector Augmented-Wave Method. *Phys. Rev. B: Condens. Matter Mater. Phys.* **1994**, *50*, 17953−17979.
(52) Kresse, G.; Joubert, D. From Ultrasoft Pseudopotentials to the Projector Augmented-Wave Method. *Phys. Rev. B: Condens. Matter Mater. Phys.* **1999**, *59*, 1758−1775.
(53) Kresse, G.; Hafner, J. *Ab Initio* Molecular Dynamics for Liquid Metals. *Phys. Rev. B: Condens. Matter Mater. Phys.* **1993**, *47*, 558−561.
(54) Kresse, G.; Hafner, J. *Ab Initio* Molecular-Dynamics Simulation of the Liquid-Metal−amorphous-Semiconductor Transition in Germanium. *Phys. Rev. B: Condens. Matter Mater. Phys.* **1994**, *49*, 14251−14269.
(55) Kresse, G.; Furthmüller, J. Efficient Iterative Schemes for *Ab Initio* Total-Energy Calculations Using a Plane-Wave Basis Set. *Phys. Rev. B: Condens. Matter Mater. Phys.* **1996**, *54*, 11169−11186.
(56) Perdew, J. P.; Burke, K.; Ernzerhof, M. Generalized Gradient Approximation Made Simple. *Phys. Rev. Lett.* **1996**, *77*, 3865−3868.
(57) Grimme, S. Semiempirical GGA-Type Density Functional Constructed with a Long-Range Dispersion Correction. *J. Comput. Chem.* **2006**, *27*, 1787−1799.
(58) Henkelman, G.; Jónsson, H. Improved Tangent Estimate in the Nudged Elastic Band Method for Finding Minimum Energy Paths and Saddle Points. *J. Chem. Phys.* **2000**, *113*, 9978−9985.
(59) Monkhorst, H. J.; Pack, J. D. Special Points for Brillouin-Zone Integrations. *Phys. Rev. B* **1976**, *13*, 5188−5192.
(60) Momma, K.; Izumi, F. *VESTA 3* for Three-Dimensional Visualization of Crystal, Volumetric and Morphology Data. *J. Appl. Crystallogr.* **2011**, *44*, 1272−1276.
(61) Popov, Z. I.; Mikhaleva, N. S.; Visotin, M. A.; Kuzubov, A. A.; Entani, S.; Naramoto, H.; Sakai, S.; Sorokin, P. B.; Avramov, P. V. The Electronic Structure and Spin States of 2D graphene/VX_2 (X = S, Se) Heterostructures. *Phys. Chem. Chem. Phys.* **2016**, *18*, 33047−33052.
(62) Gauzzi, A.; Sellam, A.; Rousse, G.; Klein, Y.; Taverna, D.; Giura, P.; Calandra, M.; Loupias, G.; Gozzo, F.; Gilioli, E.; et al. Possible Phase Separation and Weak Localization in the Absence of a Charge-Density Wave in Single-Phase 1T-VS_2. *Phys. Rev. B: Condens. Matter Mater. Phys.* **2014**, *89*, 235125.
(63) Wang, W.; Sun, Z.; Zhang, W.; Fan, Q.; Sun, Q.; Cui, X.; Xiang, B. First-Principles Investigations of Vanadium Disulfide for Lithium and Sodium Ion Battery Applications. *RSC Adv.* **2016**, *6*, 54874−54879.
(64) Persson, K.; Sethuraman, V. A.; Hardwick, L. J.; Hinuma, Y.; Meng, Y. S.; van der Ven, A.; Srinivasan, V.; Kostecki, R.; Ceder, G. Lithium Diffusion in Graphitic Carbon. *J. Phys. Chem. Lett.* **2010**, *1*, 1176−1180.

DOI: 10.1021/acs.jpcc.7b07630
J. Phys. Chem. C 2017, 121, 24179−24184